Structure and Properties of Hybrid Poly(2-hydroxyethyl methacrylate)/SiO_2 Monoliths

Xiang-Ling Ji, Shi-Chun Jiang, Xue-Peng Qiu, De-Wen Dong, Dong-Hong Yu, Bing-Zheng Jiang

State Key Laboratory of Polymer Physics and Chemistry, Changchun Institute of Applied Chemistry, Chinese Academy of Sciences, Changchun 130022, People's Republic of China

Received 29 October 2001; accepted 4 September 2002

ABSTRACT: Hybrid poly(2-hydroxyethyl methacrylate) (PHEMA)/SiO_2 monoliths were synthesized via a sol–gel process of the precursor tetraethyl orthosilicate (TEOS) and the *in situ* free-radical polymerization of 2-hydroxyethyl methacrylate (HEMA). The weight ratio of the starting chemicals, TEOS to HEMA, was varied between 100/0 and 0/100. Structural analysis was performed by IR and NMR. The NMR results indicated that the introduction of PHEMA in the silica networks gave rise to a lower degree of condensation of TEOS. The resulting monoliths showed more than 75% transmittance in the visible region, that is, good transparency. Mechanical properties were studied with an Instron tester, and the monoliths exhibited better compressive strength and modulus than did bulk PHEMA. Surprisingly, thermogravimetric analysis (TGA) data showed greater than 50 wt % solid residue up to 700°C, possibly related to some degree of chemical crosslinking between the polymer and the silica moiety, which would greatly improve the thermal stability of such hybrid monoliths compared with a pure PHEMA.

Key words: silicas; radical polymerization; structure; properties

INTRODUCTION

During the past decade, hybrid organic–inorganic materials have rapidly become a fascinating new field in materials science.[1–16] These materials are usually prepared by the sol–gel approach, which creates homogeneous ceramics, glasses, and composites with great ranges of composition and properties at low temperatures.[17–19] The exact control provided over bulk chemical and physical properties has made these materials excellent candidates for application as both structural and functional materials.[20–22]

Polymer–silica hybrid materials have been reported on since the 1980s. Loy and colleagues prepared some bridged polysilsequioxanes that were highly porous hybrid organic–inorganic materials.[10,23] These materials exhibited potential application, by growing nanoparticles in the pore structure of dried xerogels, for nonlinear optics. Bridged bisimide polysilsequioxane xerogels were investigated by Hobson and Shea.[15] Polyimides with good mechanical and thermal properties were utilized as bridged organic moieties into inorganic matrices, and the resultant materials showed good thermal stabilities and hardness. Wilkes and colleagues extensively studied the microstructure of a hybrid poly(tetramethylene oxide)/tetraethyl orthosilicate (TEOS) system through small-angle X-ray scattering, differential scanning calorimetry, thermogravimetric analysis (TGA), solid-state NMR, tensile testing, dynamic mechanical analysis, and transmission electron microscopy, and provided a schematic microstructure for polymer–silica hybrids.[3,24]

Usually, inorganic SiO_2 monolithic glasses prepared via the sol–gel process are very fragile. Shrinkage of gel is attributed to evaporation of water, catalyst, byproducts, and solvents. Novak and coworkers synthesized some nonshrinkable inorganic–organic hybrids with only a small amount of evaporation during aging and drying.[6–9] They examined the hydrolysis and condensation of TEOS to form an inorganic SiO_2 matrix, while simultaneously eliminating unsaturated alcohols, which could then be polymerized to produce an organic phase. This route is very useful for the preparation of organic–inorganic hybrid monoliths with high SiO_2 contents.

In this study, hybrid poly(2-hydroxyethyl methacrylate) (PHEMA)/SiO_2 monoliths were prepared with

Correspondence to: X.-L. Ji (xlji@ns.ciac.jl.cn or xji@ tulane.edu).

Contract grant sponsor: Natural Science foundation of China; contract grant numbers: 29774030, 29974033, 50073024, and 90101001.

Contract grant sponsor: Youth Foundation of Jilin Province Scientific Council, Key Project of Chinese Academy of Sciences for '95' Basic Research; contract grant number: KJ952-J1-501.

Contract grant sponsor: National Basic Research Project: Macromolecular Condensed State.

Contract grant sponsor: Special Fund for Major State Research Project; contract grant number: G1999064805.

Contract grant sponsor: Special Fund of the Natural Science Foundation of China; contract grant number: 20023003.

Journal of Applied Polymer Science, Vol. 88, 3168–3175 (2003)

TABLE I
Composition

Sample	TEOS (g)	HEMA (g)	H_2O (g)	pH	DMF (mL)	BPO (mg)
A	2.0	0	0.69	3.5	2.10	0
B	1.6	0.4	0.58	3.5	1.87	2
C	1.2	0.8	0.42	3.5	1.40	4
D	0.8	1.2	0.28	3.0	0.93	6
E	0.4	1.6	0.14	3.5	0.80	8
F	0	2.0	0		0.20	10

a conventional sol–gel process. PHEMAs based on hydrogels were used as swellable matrices for the release of different classes of bioactive agents because of their biocompatibility characteristics.[25] The most successful application of PHEMA hydrogel is for hydrophilic soft contact lenses, which today are an essential commodity supported by excellent clinical results and a huge industry.[26] The aim of our as-synthesized hybrid was to combine the advantage of both

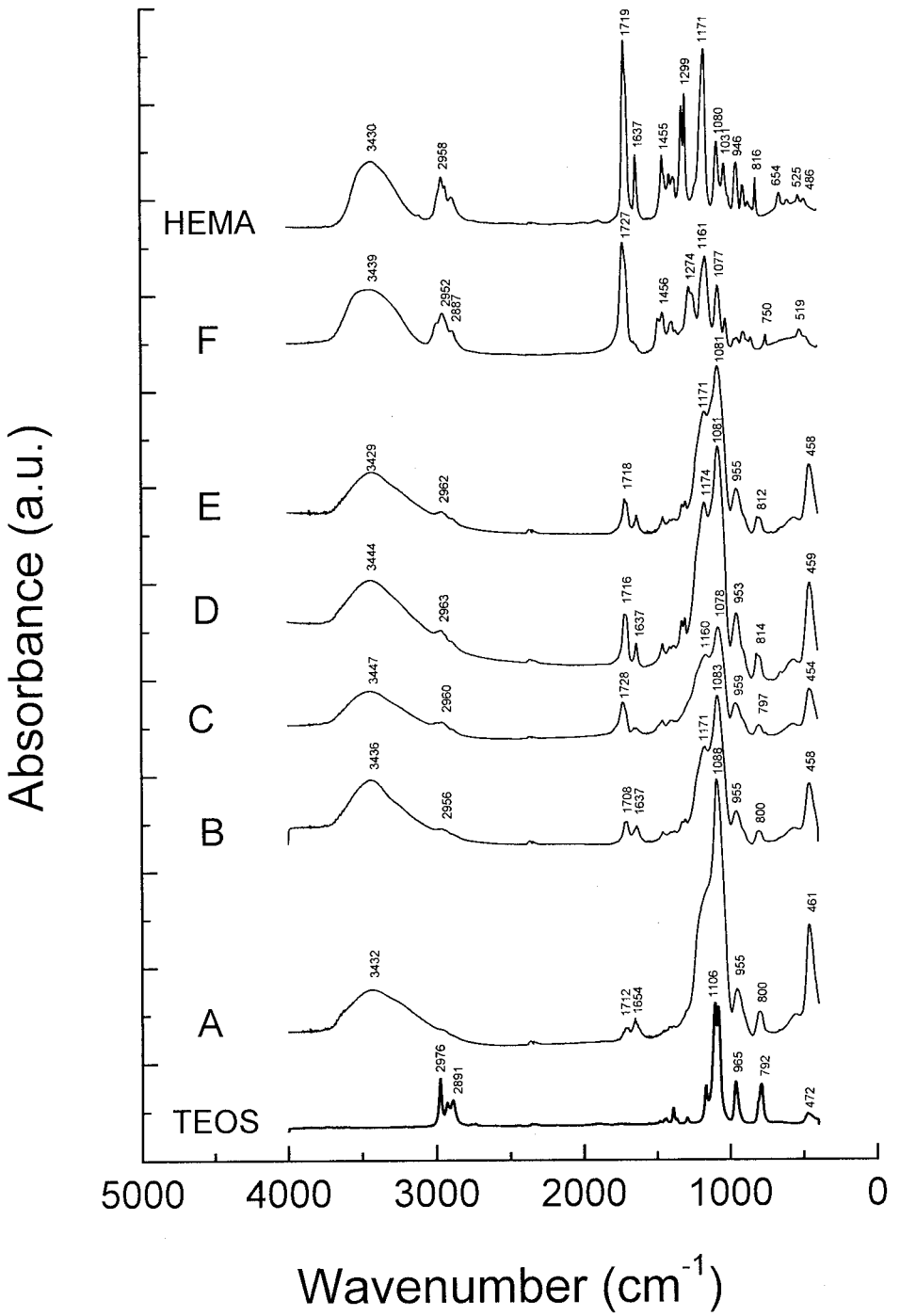

Figure 1 IR spectra for hybrids with TEOS/HEMA weight ratios of (A) 100/0, (B) 80/20, (C) 60/40, (D) 40/60, (E) 20/80, and (F) 0/100.

PHEMA and silica. The resulting monoliths, ranging from glass-reinforced polymers to polymer-toughened glass, exhibited unique properties.

EXPERIMENTAL

Table I lists the compositions of the initial chemicals. All of the chemicals were used without further purification. TEOS, 2-hydroxyethyl methacrylate (HEMA), water, and benzoyl peroxide (BPO) were dissolved in dimethylformamide (DMF) under stirring. The pH value was adjusted to about 3.5 through the addition of 1*M* HCl, and the mixture was reacted for 8–36 h until the sol–gel transition. The weight ratio of TEOS to HEMA was varied from 100/0 to 0/100. The gel was aged and dried at ambient temperature for a few weeks, and then, a heat treatment was carried out at 70–100°C for 2 days. The resulting specimens were transparent, colorless, and stiff monoliths. Hydrolysis and condensation of the precursor TEOS formed a silica network. HEMA dispersed in this network was initiated by BPO to become PHEMA.

IR spectra were recorded on a Bio-Rad FTS-135 Fourier transform infrared spectrometer (Bio-Rad Corp., USA) in the range 4000–400 cm^{-1} with the conventional KBr method. Solid-state NMR experiments were performed with a UNITY-400 (Varian Inc., USA) instrument, and measurement was done with ground powders. A UV-300 (Shimadzu Corp., Japan) ultraviolet spectrophotometer was used with wavelengths from 200 to 800 nm. We prepared cylindrical specimens, with diameters of 20 mm and thicknesses more than 10 mm, by polishing the monoliths, and the compression test was carried out on an Instron-1121 tester (Instron Corp., USA) at room temperature (23°C) with a crosshead speed of 50 mm/min. TGA was recorded on a PerkinElmer TGA-7 instrument (PerkinElmer Analytical Instruments, USA) under a nitrogen atmosphere from room temperature to 700°C at a heating rate of 10°C/min.

RESULTS AND DISCUSSION

Structural analysis

IR analysis

Figure 1 shows the IR spectra for the hybrids. As a reference, pure SiO_2 monolith exhibited main peaks at 3432(s), 1712(w), 1654(w), 1088(s), 955(m), 800(m), and 461(m) cm^{-1}. The band at 3432 cm^{-1} [Fig. 1(A)] was assigned to hydroxyl in silica silanol (Si—OH) groups. Bands related to different motions of Si—O—Si were shown at 1088, 800, and 461 cm^{-1}. The peak at 955 cm^{-1} corresponded to the stretching vibrations of Si—OH.[27]

In the high-frequency region (~3400 cm^{-1}), PHEMA had a wide and strong band centered at 3429 cm^{-1} [Fig. 1(F)] assigned to the OH stretching vibrations and due to the wide variety of hydrogen bonding between hydroxyl groups. Residual bulk water molecules could not be found because of the absence of bands at 2130 and 1650 cm^{-1} (H—O—H bending vibrations) and at about 700 cm^{-1}. In the region 1650–1800 cm^{-1}, a very strong and sharp peak at 1727 cm^{-1} corresponded to the stretching vibrations of carbonyl (C═O) groups. The band located at 1160 cm^{-1} was attributed to the stretching vibrations of C—O and proved the existence of ester groups in PHEMA. The band between 2600 and 3100 cm^{-1} was associated with the symmetric and antisymmetric C—H stretching vibrations of CH_2 and CH_3 groups. Detailed information is listed in Table II. These results are identical to those reported in the literature.[28]

TABLE II
Spectral Band Assignments for PHEMA

Frequency (cm^{-1})	Possible assignment
3439	ν (O–H)
2952	ν_{as} (CH_2, CH_3)
2887	ν_s (CH_2, CH_3)
1727	ν (C═O)
1456–1486	δ (CH_2)
1365–1390	CH_2 twist and rock
1252–1274	δ OH
1160	ν (C–O)
1077	ν (C–O–C)
750	ν (–C–O–)

The hybrid samples exhibited some characteristic vibrations of both SiO_2 and PHEMA, such as Si—O—Si, C═O, and COOR. The peak position related to hydroxyl (OH) groups exhibited a slight shift to a higher frequency with the addition of PHEMA, for example, at 3436, 3447, and 3444 cm^{-1} for samples B, C, and D, respectively; meanwhile, sample E exhibited a sudden decrease to a lower wavenumber at 3429 cm^{-1}. Certainly, the increase of PHEMA content resulted in stronger bands between 1630 and 1730 cm^{-1}, and carbonyl stretching vibrations at 1705–1730 cm^{-1} increased gradually too. In a broad band between 1000 and 1200 cm^{-1}, two peaks occurred. One, at 1160–1173 cm^{-1}, came from the stretching vibrations of C—O in ester groups; another, at 1080 cm^{-1} gathering with 800–815 and 455 cm^{-1}, was attributed to the characteristic vibrations of Si—O—Si in silica. Both samples B and C kept three peaks at 1080, 800, and 455 cm^{-1} with no obvious shift. However, samples D and E showed peaks at 812 and 814 cm^{-1}, respectively, which was perhaps related to the chemical bonds between PHEMA and silica (Si—O—C).

For the HEMA monomer, the C═C stretching vibrations were located at 1637 cm^{-1}; for pure PHEMA, no such a peak was observed, which indicated complete polymerization. However, samples B, C, D, and E all exhibited very weak peaks at 1637 cm^{-1}, which

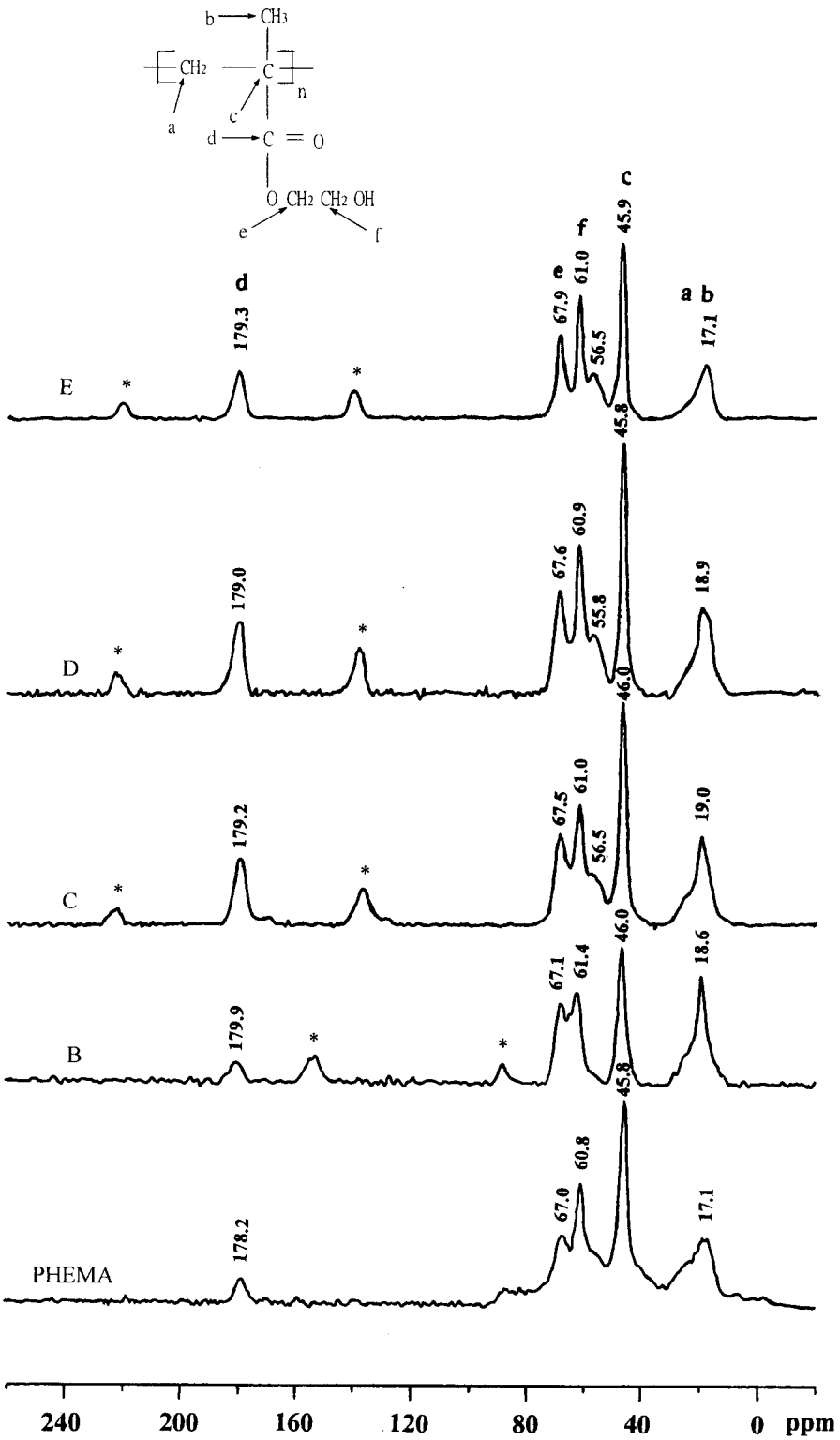

Figure 2 Solid-state ^{13}C CP–MAS NMR spectra with TEOS/HEMA weight ratios of (B) 80/20, (C) 60/40, (D) 40/60, and (E) 20/80. *Spinning side bands.

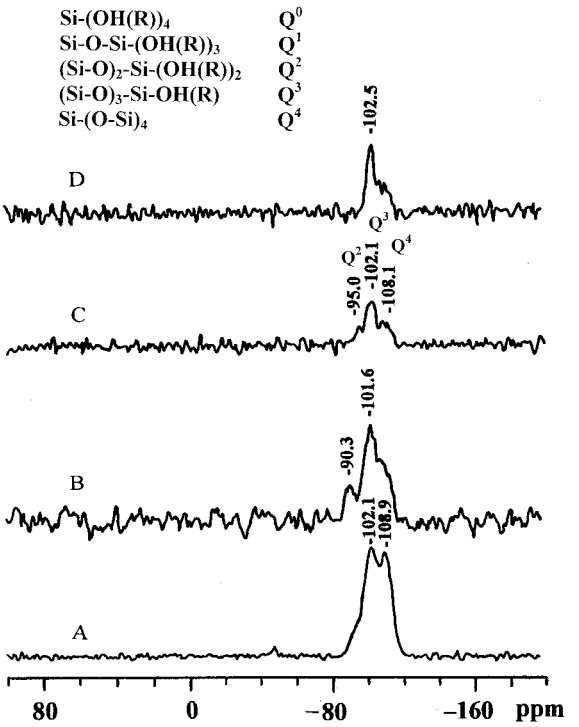

Figure 3 Solid-state ^{29}Si MAS NMR spectra with TEOS/HEMA weight ratios of (A) 100/0, (B) 80/20, (C) 60/40, and (D) 40/60.

implied the existence of C═C, that is, residual HEMA monomer. The main reason stemmed from the occurrence of network formation before free-radical polymerization.

Solid-state NMR spectroscopy

Solid-state ^{13}C cross-polarity/magic-angle spinning (CP–MAS) NMR spectroscopy. SiO_2-based hybrids were examined by solid-state NMR spectroscopy.[10,12,15,23,29] Solid-state NMR spectroscopy is a very useful technique for characterizing these interactable hybrid materials. For pure PHEMA, there were six kinds of carbons, as indicated in Figure 2. The peaks at 178.2 and 45.8 ppm were assigned to the carbons of ester and *tert*-butyl, respectively. The carbon of alcohol attached to the ester group showed its signal at 67.5 ppm, and another carbon attached to a hydroxy group displayed a peak at 60.8 ppm. A broad peak at 17.1 ppm was assigned to a combination of CH_2 and CH_3 to the carbon of *tert*-butyl. Hybrid samples only exhibited some changes in intensity at about 67 ppm. With increasing SiO_2 content, the intensity at 67 ppm gradually increased, which was probably caused by a changeable chemical environment, that is, a confined SiO_2 network. Samples C, D, and E all exhibited shoulders, at 56.5, 55.8, and 56.5 ppm, respectively. A detailed study is in progress. High SiO_2 content (samples B, C, and D) gave rise to a shift to upfield, for example, from 17.1 to 18.6, 19.0, and 18.9 ppm followed an increase in intensity and a narrow band. There was little evidence for residual HEMA monomer because of an absence of peaks in the range 100–150 ppm.

Solid-state ^{29}Si magic-angle spinning (MAS) NMR spectroscopy. ^{29}Si-NMR spectroscopy was used to evaluate the degree of condensation (the relative number of siloxane bonds to each silicon atom) in the networks. Five possible types of silicon atoms with different degrees of condensation existed in these TEOS system. Here, Q^n stands for different kinds of silicon atoms, where $n = 0$, 1, 2, 3, or 4 and is equal to the number of silicon atoms with how many siloxane bonds. Q^0 represents a silicon atom with no siloxane linkages and would be expected to occur in the free monomer; Q^1, Q^2, Q^3, and Q^4 denote silicon atoms with one, two, three, and four siloxane bonds. In Figure 3, the peak at 108–109 ppm came from Q^4, the one at 101–102 ppm corresponded to Q^3, and the peak at 90–95 ppm was related to Q^2. After the deconvolution of peaks, we calculated the degree of condensation semiquantitatively according to eq. (1):

$$\text{Degree of condensation} = [1.0(\%\ \text{Area}\ Q^1) + 2.0(\%\ \text{Area}\ Q^2) + 3.0(\%\ \text{Area}\ Q^3) + 4.0(\%\ \text{Area}\ Q^4)]/4.0 \quad (1)$$

Table III lists the degree of condensation of the hybrid samples. The SiO_2 monolith showed a higher Q^4 value when compared with hybrid samples. The addition of polymers resulted in a decrease in Q^4, an increase in Q^3, and a presence of Q^2 for samples B and C. The appearance of Q^2 for samples B and C was in accordance with the IR spectra, that is, a decrease in intensity at 1083 and 1078 cm^{-1} corresponding to Si—O—Si vibrations. However, the introduction of polymers inhibited the formation of a three-dimensional network to some extent. Sample D reached its gel point in a shorter time compared with samples B and C, and it showed a high degree of condensation and no Q^2 but a high Q^3 and Q^4. The reason was perhaps related to the pH, which was a little lower for sample D, which gave rise to rapid hydrolysis and condensation and facilitated the achievement of a high degree of condensation.

TABLE III
Degree of Condensation

Sample	Q^2 (%)	Q^3 (%)	Q^4 (%)	Degree of condensation (%)
A	0	52.2	47.8	87.4
B	15.3	55.1	29.6	78.6
C	17.8	53.4	28.8	77.8
D	0	66.7	33.3	83.3

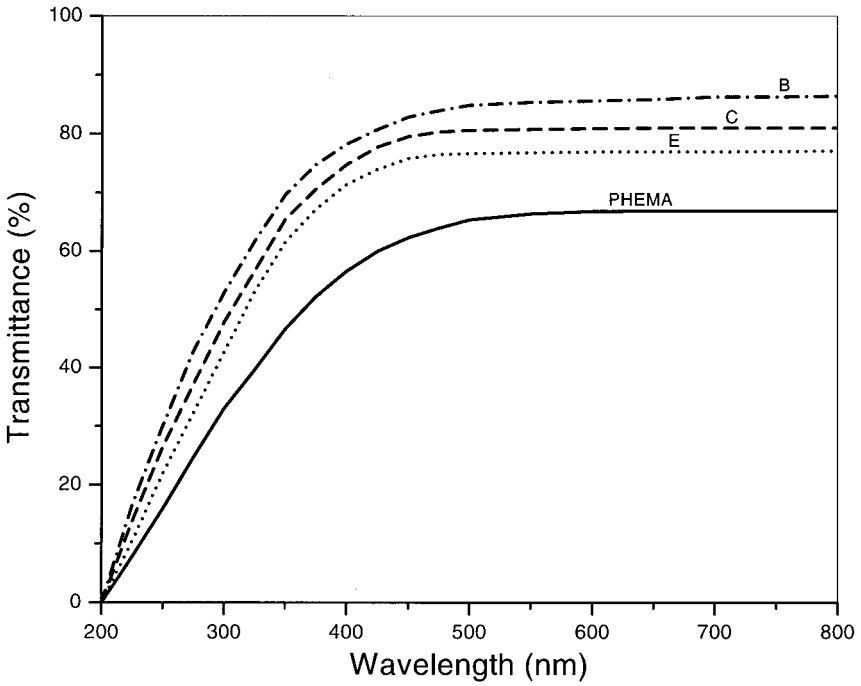

Figure 4 UV–vis spectra of PHEMA (thickness = 3.22 mm) and samples B, C, and E (thickness = 3.30 mm) with TEOS/HEMA weight ratios of (B) 80/20, (C) 60/40, and (E) 20/80.

Transparency

The ultraviolet–visible (UV–vis) spectra are shown in Figure 4. A PHEMA sheet with a thickness of 3.22 mm exhibited its transmittance at less than 60% in the range 200–400 nm and at more than 65% in the visible region. However, hybrids monoliths (with thicknesses of 3.30 mm) exhibited their transmittance at as high as 75% in the range 400–800 nm, which suggested a good transparency in the visible region. Higher SiO_2 contents led to a slight increase in transmittance.

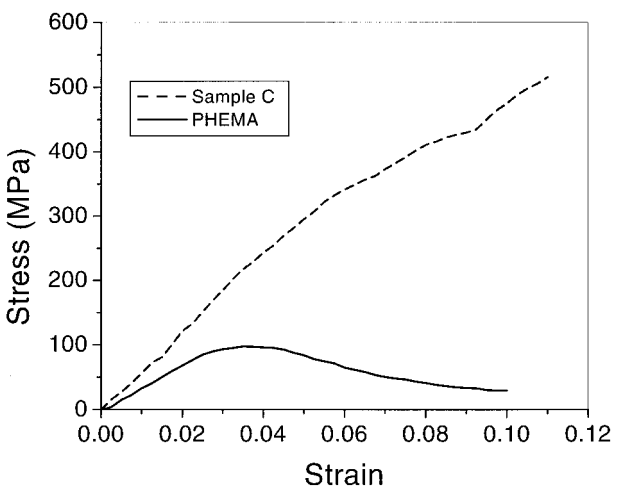

Figure 5 Compression stress–strain curves for PHEMA and sample C with 27 wt % silica.

Mechanical properties

Compression properties were carried out on an Instron tester. Figure 5 shows the stress–strain curves. The compressive strength of a hybrid monolith (sample C) increased with increasing strain and up to 515 MPa at 0.11 of strain until the specimen broke. However, no obvious yield point occurred. As a reference,

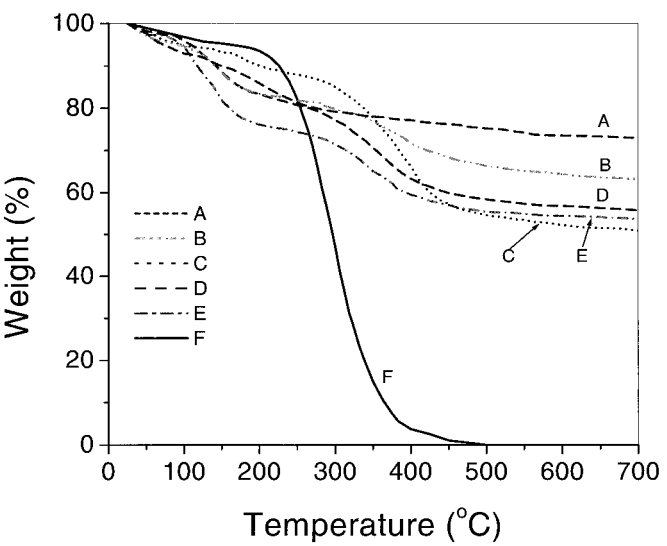

Figure 6 TGA profiles under nitrogen atmosphere: (A) SiO_2, (B) 50/50 SiO_2/PHEMA, (C) 27/73 SiO_2/PHEMA, (D) 14/86 SiO_2/PHEMA, (E) 5.5/94.5 SiO_2/PHEMA, and (F) PHEMA.

PHEMA showed its yield strength at about 97 MPa and showed a similar strain at break. The hybrid monoliths definitely exhibited better compression properties than pure PHEMA. After a linear fit to the initial region, the compressive modulus was 6.18 ± 0.10 GPa for the hybrids and 3.52 ± 0.08 GPa for PHEMA.

Thermal stability

Figure 6 shows the TGA curves under a N_2 atmosphere for the PHEMA/SiO_2 hybrids. For PHEMA [Fig. 6(F)], from room temperature to 200°C, the weight loss of 7% was due to a little solvent (DMF) and unreacted monomer HEMA; between 200 and 400°C, weight loss was so high, up to 91%, and relatively the fastest rate of decomposition occurred at 296°C. This may have been due to the thermal depolymerization of the polyacrylates: when a sample was heated to its depolymerization temperature, polymers started to decompose very rapidly during a short period. PHEMA degraded completely at 500°C.

SiO_2 monolith prepared via the sol–gel route, had a weight loss of about 15% at 200°C and about 29% at 700°C. From 200 to 700°C, a weight loss of 14% covered the decomposition of SiO_2. Figure 6(A,F) implies that before 200°C, the weight loss of both SiO_2 and PHEMA basically came from residual solvents, water, catalysts, and so on.

Figure 6(B–E) shows the TGA traces of the hybrid PHEMA/SiO_2. There were three stages: the first stage at about 40°C corresponding to a mixture of alcohol and water, the second at 140–200°C including residual DMF and unreacted HEMA, and the third one located above 340°C. Table IV lists the weight loss between 200 and 700°C ($W_1 - W_2$), where W_1 and W_2 are the weight percentages of the specimen at 200°C and 700°C, respectively. At 700°C the solid residue of samples B, C, D, and E were 63, 50, 53, and 54%, respectively. PHEMA contents in the hybrids, calculated from the initial compositions, were about 50, 73, 86, and 94.5%, respectively. The previous data indicated that some of PHEMA existed in the hybrids up to 700°C. These results are quite different from reported systems such as polyacrylonitrile/SiO_2, poly(allyl methacrylate)/silica, and polyamide/silica.[30–32] This is possibly because of the condensation reaction between OH groups in PHEMA chains and OH groups in SiO_2 networks, which resulted in the PHEMA chains being grafted to the SiO_2 networks; that is, both the PHEMA and SiO_2 were connected with chemical bonds and produced chemical hybridization. However, this kind of structure improved thermal stability effectively.

TABLE IV
TGA Data

Sample	A	B	C	D	E	F
TEOS/HEMA	100/0	80/20	60/40	40/60	20/80	0/100
SiO_2/PHEMA	100/0	50/50	27/73	14/86	5.5/94.5	0/100
W_1 (%, 200°C)	85	83	90	76	82	93
W_2 (%, 700°C)	71	63	50	53	54	0
W_1-W_2 (%)	14	20	40	23	28	93

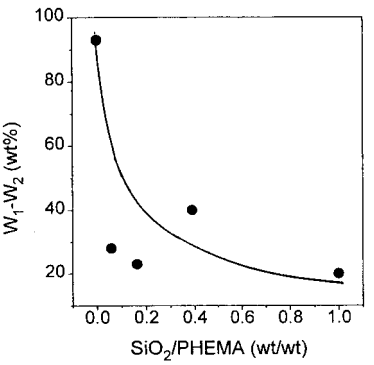

Figure 7 Variation of percentage weight loss between 200 and 700°C ($W_1 - W_2$) with the SiO_2/PHEMA weight ratio in the hybrid.

The percentage weight loss from 200 to 700°C ($W_1 - W_2$) versus the SiO_2/PHEMA weight ratio is plotted in Figure 7. With increasing SiO_2 content, the weight loss of the hybrids decreased, even though the hybrids contained a small amount of SiO_2, such as sample E with of 5.5 wt % SiO_2, the thermal stability increased greatly.

CONCLUSIONS

Hybrid PHEMA/SiO_2 monoliths were prepared via the sol–gel approach and *in situ* polymerization. The introduction of PHEMA led to a decrease in the degree of condensation of TEOS to some extent. The hybrids exhibited some characteristic molecular structure of both PHEMA and SiO_2. These hybrid monoliths exhibited good transparency, more than 75% transmittance in the visible region, and better compressive strengths and moduli than bulk PHEMA. Surprisingly, TGA data showed above 50 wt % solid residue up to 700°C, possibly related to some extent of chemical crosslinking between the polymer chains and the silica surface, which greatly improved the thermal stability of the hybrid monoliths compared with pure PHEMA.

References

1. Judeinstein, P.; Sanchez, C. J Mater Chem 1996, 6, 511.
2. Philipp, G.; Schmidt, H. J Non-Cryst Solids 1984, 63, 283.
3. Huang, H.-H.; Orler, B.; Wilkes, G. L. Macromolecules 1987, 20, 1322.
4. Huang, H.-H.; Wilkes, G. L.; Carlson, J. G. Polymer 1989, 30, 2001.

5. Noell, J. L. W.; Wilkes, G. L.; Mohanty, D. K. J Appl Polym Sci 1990, 40, 1177.
6. Ellsworth, M. W.; Novak, B. M. J Am Chem Soc 1991, 113, 2756.
7. Novak, B. M.; Davies, C. Macromolecules 1991, 24, 5481.
8. Novak, B. M.; Ellsworth, M. W. Mater Sci Eng A 1993, 162, 257.
9. Ellsworth, M. W.; Novak, B. M. Chem Mater 1993, 5, 839.
10. Loy, D. A.; Shea, K. J. Chem Rev 1995, 95, 1431.
11. Schubert, U.; Husing, N.; Lorenz, A. Chem Mater 1995, 7, 2010.
12. Loy, D. A.; Jamison, G. M.; Baugher, B. M.; Myers, S. A.; Assink, R. A.; Shea, K. J. Chem Mater 1996, 8, 656.
13. Jackson, C. L.; Bauer, B. J.; Nakatani, A. I.; Barnes, J. D. Chem Mater 1996, 8, 727.
14. Wen, J.; Wilkes, G. L. Chem Mater 1996, 8, 1667.
15. Hobson, S. T.; Shea, K. J. Chem Mater 1997, 9, 616.
16. Hybrid Organic–Inorganic Composites; Mark, J. E.; Lee, C. Y. C.; Bianconi, P. A., Eds.; ACS Symposium Series 585; American Chemical Society: Washington, DC, 1995; p 1.
17. Ulrich, D. R. Chemtech 1988, 18, 242.
18. Ulrich, D. R. J Non-Cryst Solids 1988, 100, 174.
19. Brinker, C. J.; Scherrer, G. Sol–Gel Science: The Physics and Chemistry of Sol–Gel Processing; Academic: New York, 1990; pp. 498–506.
20. Shea, K. J.; Loy, D. A. Chem Mater 2001, 13, 3306.
21. Walcarius, A. Chem Mater 2001, 13, 3351.
22. Sanchez, C.; Soler-Illia, G. J. de A. A.; Ribot, F.; Labot, T.; Mayer, C. R.; Cabuil, V. Chem Mater 2001, 13, 3061.
23. Loy, D. A.; Jamison, G. M.; Baugher, B. M.; Russick, E. M.; Assink, R. A.; Prabakar, S.; Shea, K. J. J Non-Cryst Solids 1995, 186, 44.
24. Betrabet, C. S.; Wilkes, G. L. Chem Mater 1995, 7, 535.
25. Agarwal, S.; Sumana, G.; Gupta, D. C. J Appl Polym Sci 1997, 66, 267.
26. Chirila, T. V.; Constable, I. J.; Crawford, G. J.; Vijayasekaran, S.; Thompson, D. E.; Chen, Y.-C.; Fletcher, W. A.; Griffin, B. J. Biomaterials 1993, 14, 26.
27. Almeida, R. M.; Pantano, C. G. J Appl Phys 1990, 68, 4225.
28. Perova, T. S.; Vij, J. K.; Xu, H. Colloid Polym Sci 1997, 275, 323.
29. Simonutti, R.; Comotti, A.; Negroni, F.; Sozzani, P. Chem Mater 1999, 11, 822.
30. Wei, Y.; Yang, D.; Tang, L. Makromol Chem Rapid Commun 1993, 14, 273.
31. Wei, Y.; Bakthavatchalam, R.; Whitecar, C. I. Chem Mater 1990, 2, 337.
32. Wang, S.; Amad, Z.; Mark, J. E. Polym Bull 1993, 31, 323.